Chapter 6

Physics Studies with Heavy Ions

6.1 Benchmark Channel: $\mathrm{PbPb} \to Q\overline{Q} + X \to \mu^+\mu^- + X$

The measurement of the charmonium (J/ψ, $\psi^{'}$) and bottomonium (Υ, $\Upsilon^{'}$, $\Upsilon^{''}$) resonances in PbPb collisions at $\sqrt{s_{_{NN}}}$ = 5.5 TeV provides crucial information on the many-body dynamics of high-density QCD matter. First, the step-wise suppression of heavy quarkonia production is generally agreed to be one of the most direct probes of Quark-Gluon-Plasma formation. Lattice QCD calculations of the heavy-quark potential indicate that colour screening dissolves the ground-state charmonium and bottomonium states, J/ψ and Υ, at $T_{\rm diss} \approx 2 \cdot T_{\rm crit}$ and $4 \cdot T_{\rm crit}$, respectively. While the interest of charmonia production studies in heavy-ion collisions is well established from measurements done at the SPS and at RHIC, the clarification of some important remaining questions requires equivalent studies of the Υ family, only possible at the LHC energies. Second, the production of heavy-quarks proceeds mainly via gluon-gluon fusion processes and, as such, is sensitive to saturation of the gluon density at low-x in the nucleus ("Colour Glass Condensate"). Measured departures from the expected "vacuum" (proton-proton) quarkonia cross-sections in PbPb collisions at LHC will thus provide valuable information not only on the thermodynamical state of the produced partonic medium, but also on the initial-state modifications of the nuclear parton (especially, gluon) distribution functions.

This first CMS heavy-ion physics analysis focuses on the measurement of the heavy-quarkonia cross-sections in PbPb collisions at $\sqrt{s_{_{NN}}}$ = 5.5 TeV, via their dimuon decay channel. The generation of realistic signals and backgrounds, the dimuon reconstruction algorithm and the trigger, acceptance and efficiency corrections are discussed. The obtained dimuon mass resolutions, the signal over background as well as the expected yields in one-month PbPb running are presented.

6.1.1 Simulation of physics and background processes

The relatively low Υ production rates ($\sim 10^{-4}$ per PbPb event) and the large number of particles to track in heavy-ion collisions make it very expensive computationally to use a full nucleus-nucleus event generator (such as *e.g.* HIJING [168]) with detailed detector simulation and reconstruction to obtain a statistically significant sample of signal events. Instead, a combination of fast and slow simulations are used in this analysis. The input signal and backgrounds are obtained from realistic distributions: NLO pQCD for heavy-quark production processes, and HIJING for the soft background, constrained by extrapolations from lower energy heavy-ion data. A full detector and trigger simulation plus reconstruction are carried out for a few 10^7 events with single and pair particles of the different types and the corre-

sponding response functions (acceptances, resolutions, efficiencies, etc) are parameterised in a fast MC, used to obtain the final fully corrected yields. The response functions are cross-checked by comparing the final dimuon spectra obtained with the fast MC against 5×10^5 PbPb HIJING events fully simulated and reconstructed in the detector.

The quarkonium production cross sections in PbPb are obtained from NLO pp calculations at $\sqrt{s}$ = 5.5 TeV made in the colour evaporation model (CEM) [169], using MRST PDF modified with the EKS98 prescription for nuclear shadowing [170], with renormalisation and factorisation scales $\mu_R = \mu_F = m_Q$, and scaled by A^2 ($A = 208$ for Pb). The resulting (impact-parameter averaged) inclusive quarkonia production cross sections are: $B_{\mu\mu}\,\sigma_{Q\overline{Q}}$ = 49000, 900, 300, 80, 45 μb for J/ψ, $\psi^{'}$, Υ, $\Upsilon^{'}$, and $\Upsilon^{''}$, respectively. The NLO double-differential $d^2\sigma/dp_T d\phi$ distributions of J/ψ and Υ are also used for the other states within each quarkonium family.

The two main sources of background in the dimuon invariant mass spectrum are:

1. Uncorrelated decays of **charged pions and kaons**, which represent about 90% of the produced charged particles. This source was simulated using input pion and kaon $d^2N/dp_T d\eta$ distributions from HIJING, absolutely normalised to give $dN_{ch}/d\eta|_{\eta=0}$ = 2500 (*low*) and 5000 (*high*) multiplicities in central PbPb. Both cases are conservative ("pessimistic") estimates, since extrapolations from RHIC data indicate that $dN_{ch}/d\eta|_{\eta=0} \approx$ 2000 at the LHC.

2. The other source of background muons are **open heavy flavour** (D, B mesons) decaying a few mm away from the interaction vertex. The probability to produce at least one muon at the end of the decay chain of charm (bottom) quarks is ∼18% (38%) according to PYTHIA 6.025. The double differential (p_T, η) cross-sections are obtained from pp NLO calculations (with CTEQ5M1 PDF, and $\mu_R = \mu_R = m_Q$), which give $\sigma_{c\bar{c},b\bar{b}}$ = 7.5, 0.2 mb [169], scaled by the nuclear overlap function, $\langle T_{PbPb}(b = 0\,\text{fm})\rangle$ = 30.4 mb^{-1}, to obtain the expected yields in central PbPb collisions.

A fast MC simulation equivalent to $5 \cdot 10^7$ PbPb events has been carried out superimposing the decay dimuon from the five quarkonium resonances on top of the background from the combinatorial decays of π, K and open heavy flavour. Each muon track (with a given momentum, pseudorapidity, charge and origin) is weighted by a factor that takes into account the corresponding detector acceptance, as well as trigger and reconstruction efficiency for the two event multiplicities considered (see next section).

6.1.2 Reconstruction and analysis

6.1.2.1 Dimuon trigger and acceptance

The response of the CMS detector to muons (as well as long-lived punchthrough pions and kaons reaching the muon chambers) is parameterised by 2-dimensional p, η acceptance and trigger tables. The particles are fully tracked in CMS using GEANT4 from the vertex to the chambers. Each track is accepted or rejected according to the Level-1,2 heavy-ion dimuon trigger criteria [7] and the corresponding efficiencies, $\epsilon^{LVL1}_{trig}(p,\eta)$ and $\epsilon^{LVL2}_{trig}(p,\eta)$, are computed. Trigger efficiencies are of the order of ∼90% for those μ reaching the muon

chambers. The J/ψ and Υ acceptances are shown as a function of p_T in Fig. 6.1, for two η ranges: full detector and central barrel. Because of its relatively low mass, low energy J/ψ's ($p_T \lesssim 4\,\mathrm{GeV/c}$) cannot be detected since their decay muons don't have enough energy to traverse the calorimeters and they are absorbed due to ionisation losses before reaching the muon chambers. For larger p_T values the J/ψ acceptance increases and flattens out at ∼15% for $p_T \gtrsim 12\,\mathrm{GeV/c}$. The Υ acceptance starts at ∼40% at $p_T = 0\,\mathrm{GeV/c}$ and remains constant at 15% (full CMS) or 5% (barrel) for $p_T > 4\,\mathrm{GeV/c}$. The p_T-integrated acceptance is about 1.% for the J/ψ and 21% for the Υ as obtained from our input theoretical distribution.

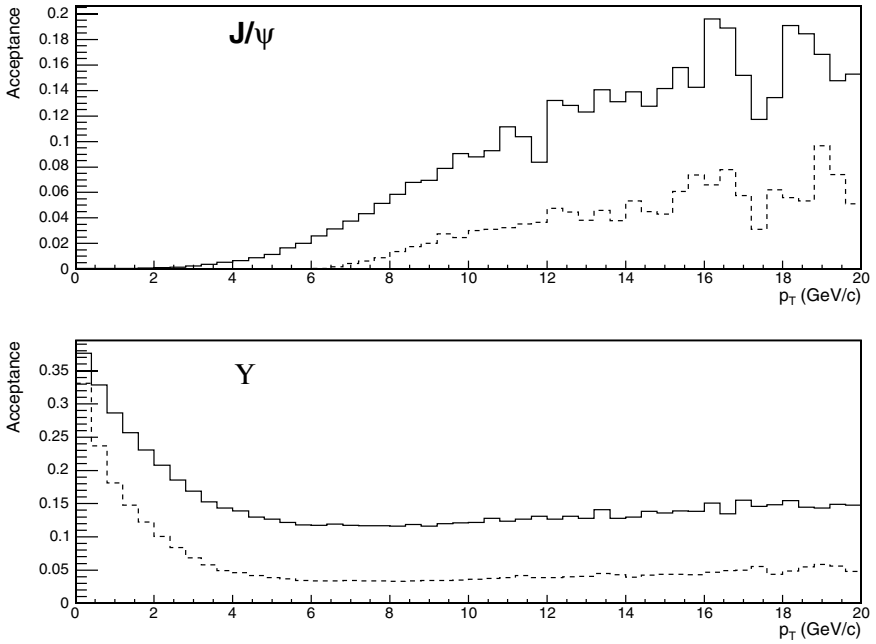

Figure 6.1: J/ψ (top) and Υ (bottom) acceptances as a function of p_T, in the full detector (barrel and endcap, $|\eta| < 2.4$, full line) and in the barrel alone ($|\eta| < 0.8$, dashed line).

6.1.2.2 Dimuon reconstruction efficiency, purity and mass resolution

The dimuon reconstruction algorithm used in the heavy-ion analysis is a version of the regional track finder based on the muons seeded by the muon stations and on the knowledge of the primary vertex, as described in [171, 172]. It is adapted to deal with the high hit occupancy of the silicon tracker in PbPb collisions. It uses the muon tracks found in the innermost muon stations to identify hits in the outer CMS tracker layer that can form the starting points (seeds) for the matching muon candidate tracks. The propagation in the tracker is performed from the outer layer towards the primary vertex, using two-dimensional parametrisation in the transverse and longitudinal planes. The final fit of trajectories is performed with a Kalman-fitter. The efficiency of a given muon pair is: $\epsilon_{pair}(p,\eta) = \epsilon_{track_1} \times \epsilon_{track_2} \times \epsilon_{vertex}$. The dependence of the Υ reconstruction efficiency on the event multiplicity was obtained from a full GEANT simulation using Υ signal dimuon embedded in HIJING PbPb events. Fig. 6.2 shows the Υ efficiency and purity (where purity is defined as the ratio of true Υ reconstructed over all Υ reconstructed) as a function of charged-particle multiplicity. In the central barrel, the dimuon reconstruction efficiency is above ∼80% for all multiplicities, whereas the purity decreases slightly with $dN_{ch}/d\eta$ but stays also above 80% even at multiplicities as high as $dN_{ch}/d\eta|_{\eta=0}$ = 6500. If (at least) one of the muons is detected in the endcaps, the effi-

ciency and purity drop due to stronger reconstruction cuts. Nonetheless, for the maximum $dN_{ch}/d\eta|_{\eta=0} \approx 2500$ multiplicities expected in central PbPb at LHC, the efficiency (purity) remains above 65% (90%) even including the endcaps.

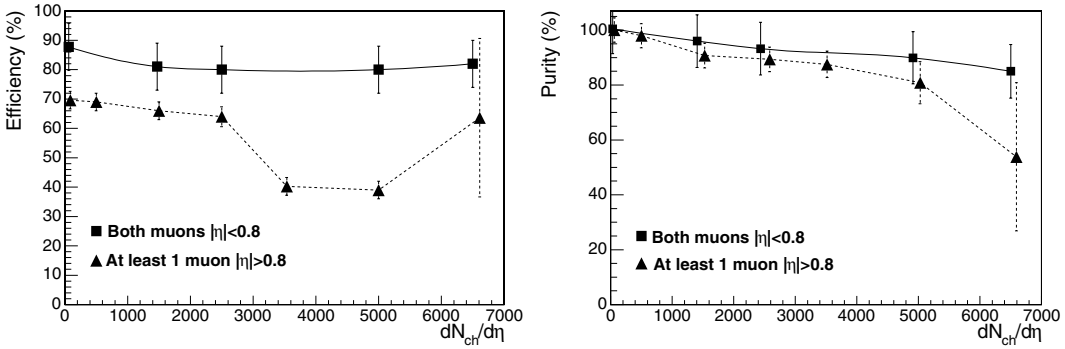

Figure 6.2: Υ reconstruction efficiency (left) and purity (right) as a function of the PbPb charged particle rapidity density, $dN_{ch}/d\eta|_{\eta=0}$.

If we only consider muon pairs in the central barrel, $|\eta| < 0.8$, the dimuon mass resolution is $\sim$54 MeV/c^2 at the Υ mass, as obtained from a Gaussian fit of the reconstructed $\mu\mu$ $m_{\rm inv}$ distribution (using a detailed MC simulation but without background). In the full pseudorapidity range, the dimuon mass resolution amounts to $\sim$1%: 35 MeV/c^2 at the J/ψ mass, and 86 MeV/c^2 at the Υ mass. These dimuon mass resolutions (the best among the LHC experiments) allow for a clean separation of the different quarkonia states. These values are used to smear the dimuon mass distribution in the fast MC studies.

6.1.3 Results

About 5×10^7 PbPb collisions were simulated. Muons passing the acceptance tables are combined to form pairs and each pair is weighted according to the trigger and reconstruction efficiencies (dependent on the momentum, η, purity and event multiplicity). Their invariant mass is calculated and smeared as described in the previous section. The obtained dimuon mass distributions are then scaled to 0.5 nb^{-1}, corresponding to the PbPb luminosity integrated in one month with average luminosity $L = 0.4 \cdot 10^{27}$ cm^{-2}s^{-1} and 50% machine operation efficiency. Fig. 6.3 shows the resulting opposite-sign mass distributions, for the *high* multiplicity case, $dN_{ch}/d\eta|_{\eta=0} = 5000$ and full acceptance (η <2.4). The different quarkonia resonances appear on top of a continuum due to several combinatorial background sources, the main ones being identified in the upper plots (h, c and b stand for $\pi + K$, charm and bottom decay muons, respectively). Since the CMS trigger and acceptance conditions treat opposite-sign and like-sign muon pairs in the same way, the uncorrelated background can be subtracted using the like-sign pairs: $N^{\rm Sig} = N^{+-} - 2\sqrt{N^{++}\,N^{--}}$, shown also in the bottom panels of Fig. 6.3.

Figure 6.4 shows the *signal* dimuon mass distributions, after background subtraction, for two different scenarios: $dN_{ch}/d\eta|_{\eta=0}$ = 5000, $|\eta| < 2.4$ ("worst" case conditions); and $dN_{ch}/d\eta|_{\eta=0}$ = 2500, $|\eta| < 0.8$ ("best" case). Except for the ψ', all quarkonia states are clearly visible. The corresponding signal-to-background ratios and yields (counted within 1σ of the resonance peaks) are collected in the Table 6.1 for one month of PbPb running.

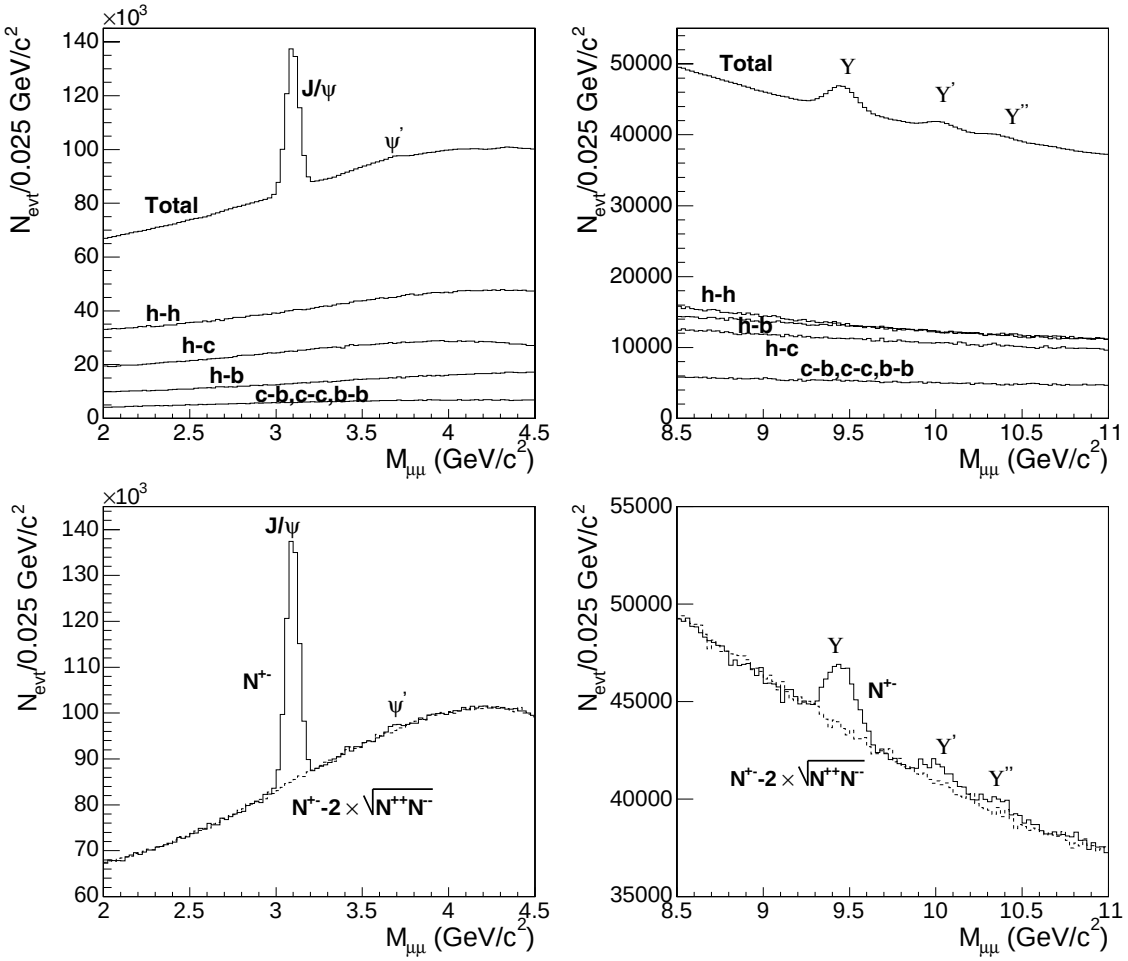

Figure 6.3: Dimuon mass distributions measured within $|\eta| < 2.4$ for PbPb events with $dN_{ch}/d\eta|_{\eta=0}$ = 5000 in the J/ψ (left) and Υ (right) mass regions. The main contributions of the background are shown in the top panels (h, c, b stand for $\pi + K$, charm, bottom decay muons resp.), while the bottom panels also show the like-sign pairs (combinatorial background).

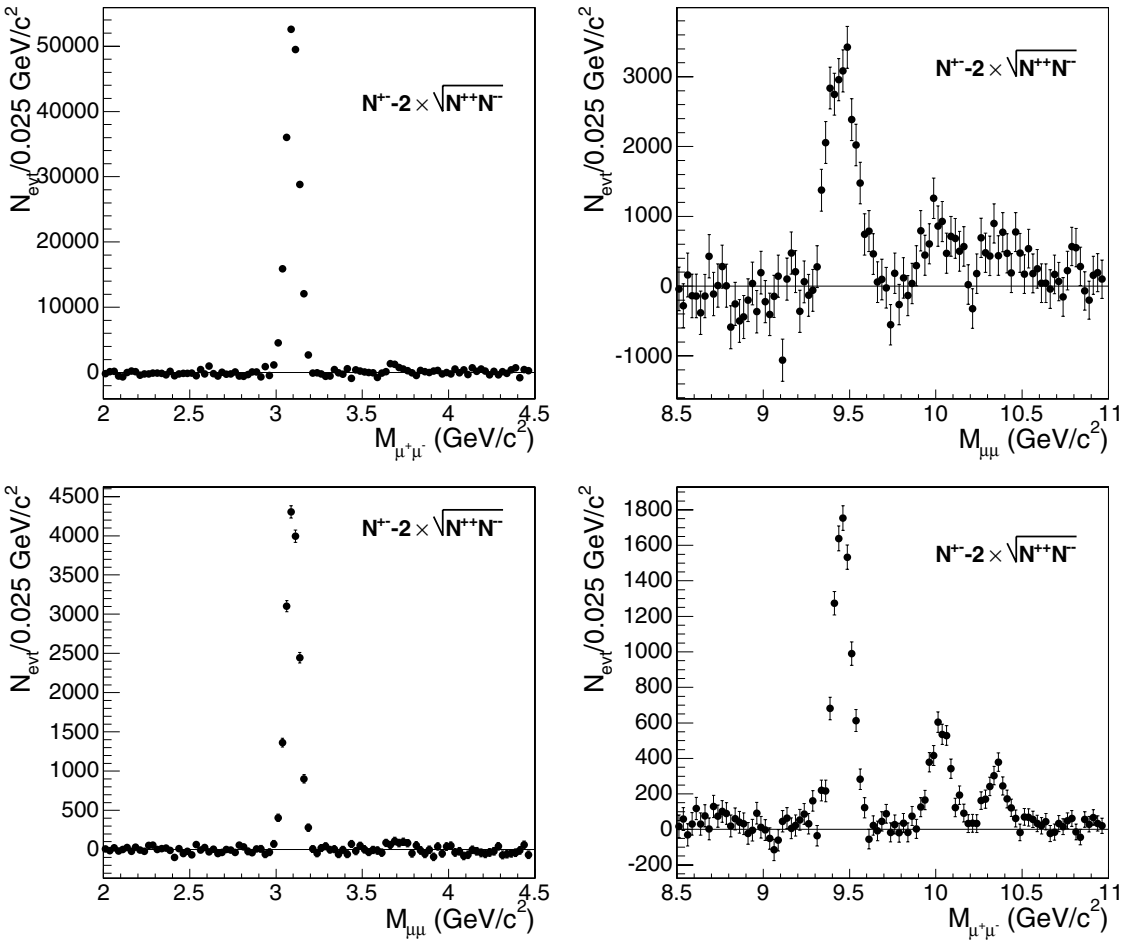

Figure 6.4: Signal dimuon mass distributions after background subtraction in the J/ψ (left) and Υ (right) mass regions expected after one month of PbPb running. Top panels for $dN_{ch}/d\eta|_{\eta=0} = 5000$ and $|\eta| < 2.4$ ("worst" case conditions); bottom panels for $dN_{ch}/d\eta|_{\eta=0} = 2500$ and $|\eta| < 0.8$ ("best" measurement conditions).

Table 6.1: Signal-to-background ratios and expected quarkonia yields in one month of PbPb running (0.5 nb^{-1} integrated luminosity) for two multiplicity scenarios and two η windows.

$dN_{ch}/d\eta\|_{\eta=0}$, $\Delta\eta$	S/B	N(J/ψ)	S/B	N(Υ)	N(Υ')	N(Υ'')
2500, $\|\eta\| < 2.4$	1.2	180 000	0.12	25 000	7300	4400
2500, $\|\eta\| < 0.8$	4.5	11 600	0.97	6400		
5000, $\|\eta\| < 2.4$	0.6	140 000	0.07	20 000	5900	3500
5000, $\|\eta\| < 0.8$	2.75	12 600	0.52	6000		

6.1.4 Conclusions

With its very broad muon acceptance and precise tracking, CMS will provide significant contributions to heavy ion physics at the LHC. Studies of quarkonium production in PbPb collisions at $\sqrt{s_{NN}}$ = 5.5 TeV, will provide crucial information on the thermodynamical state of QCD medium formed in these collisions, through the expected step-wise "melting" pattern of the different $Q\overline{Q}$ states due to colour screening. These results will also be sensitive to modifications of the low-x nuclear parton distribution functions, as expected in case of gluon saturation.

CMS can reconstruct the charmonium and bottomonium resonances, via their dimuon decay channel, with high efficiencies ($\sim$ 80%), good purity ($\sim$ 90%) and a very good dimuon mass resolution (54 MeV/c^2 at the Υ mass), when both muons are detected in the central barrel ($|\eta| < 0.8$), even in the case of exceptionally high multiplicities ($dN_{ch}/d\eta|_{\eta=0} \approx 5000$). When considering the full pseudorapidity region ($|\eta| < 2.4$), the mass resolution becomes $\sim$ 86 MeV/c^2 at the Υ, and 35 MeV/c^2 at the J/ψ, with $\sim$ 50% dimuon reconstruction efficiencies. The Υ states can be measured all the way down to p_T = 0 GeV/c with acceptances as large as 40%, while the lower rest mass of the J/ψ state and the large amount of material in the calorimeters absorbs "low" energy decay muons and prevents from measuring J/ψ's below $p_T \approx 4$ GeV/c. At high p_T (above $\sim$ 12 GeV/c for the J/ψ and $\sim$ 4 GeV/c for the Υ) the dimuon acceptance flattens out at 15%.

The large aperture of the muon detectors and the precise tracking result in a very good separation between the $Q\overline{Q}$ states in the dimuon mass distributions, and in relatively high statistics and good signal to background ratios ($S/B \approx 1(5)$, $S/B \approx 0.1(1)$ for J/ψ and Υ resp. in the full (central) rapidity range). After one month of PbPb running (0.5 nb^{-1}) we should collect $\sim$ 180 000 J/ψ and $\sim$ 25 000 Υ dimuon, enough to compare central and peripheral PbPb collisions, and to carry out some differential studies (dN/dy, dN/dp_T) which will surely contribute significantly to clarify the physics mechanisms behind the production (and "destruction") of quarkonia states in nucleus-nucleus collisions at the LHC.

Part II

CMS Physics Reach